Effect of edge-localized mode simulation on detached plasma in the divertor simulation experimental module of GAMMA 10/PDX

M. Yoshikawa, J. Kohagura, N. Ezumi, T. Kariya, R. Minami, T. Numakura, M. Hirata, S. Togo, K. Emoto, M. Sakamoto, Y. Shima, T. Okamoto, S. Takahashi, Y. Nakashima, T. Minami, S. Kobayashi[a], I. Yamadai[b], R. Yasuhara[b], H. Funaba[b], N. Kenmochi[b], D. Kuwahara[c], and H. v. d. Meiden[d]

Plasma Research Center, University of Tsukuba, Tsukuba, Ibaraki 305-8577, Japan
[a]IAE, Kyoto Univ., [b]NIFS, [c]Chubu Univ., [d]DIFFER
*e-mail: yosikawa@prc.tsukuba.ac.jp

In nuclear fusion plasmas, the study of plasma detachment is one of the most important subjects. Detached plasma decreases both heat flux and particle flux to the divertor plate. In GAMMA 10/PDX, a divertor simulation experimental module (D-module) was installed to study plasma detachment under high heat flux conditions (> 20 MW/m²). Previous studies observed the behavior of detached plasma with a suddenly changing higher density particle flux, similar to edge-localized mode (ELM), with additional heating in the core plasma region. However, the additional heating by electron cyclotron heating (ECH) and supersonic molecular beam injection (SMBI) to produce higher density and temperature of core plasma was performed in single pulse operations. In this study, we used double pulse ECH injection to investigate the behavior of the divertor simulation plasma with ELM-like intermittent higher density and temperature flux injection in the D-module. This experiment revealed the effect of intermittent higher particle fluxes on the detached simulation plasma.

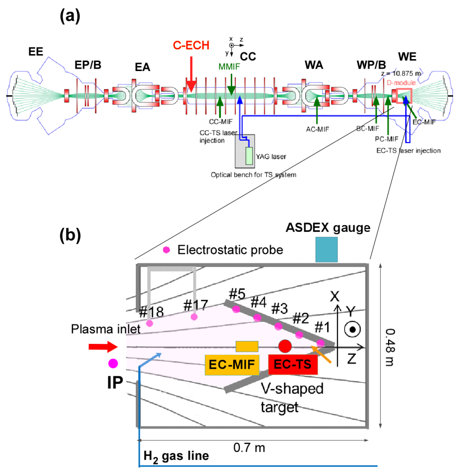

FIG. 1. Schematics of the experimental setup of GAMMA 10/PDX (a), and the divertor simulation experimental module (b).

We have been studying detached plasma mechanisms for reducing heat and particle fluxes to the divertor plate under the equivalent to ITER SOL and divertor plasma in D-module of GAMMA 10/PDX [1,2]. GAMMA 10/PDX has the main plasma confinement region of the central-cell (CC), and the escaping plasma in the west end-cell (EC) is led to the D-module for divertor simulation plasma experiments (Fig. 1). In the D-module, electron temperature and density are measured by using electrostatic probes (ESP #1-5) on the tungsten V-shaped target plate. For upstream plasma measurements in the D-module, a Thomson scattering system and a microwave interferometer system (EC-MIF) were installed. Additionally, a movable electrostatic probe was installed to observe inlet plasma parameters in front of D-module. To produce higher density and temperature particle flux into D-module, we additionally injected central electron cyclotron heating (C-ECH) in the CC. For observing the plasma radiation inside D-module, a high-speed camera system (HSCAM) with a wavelength filter for Hα or Hβ is used. Figure 1 (b) shows the D-module installed in the EC. The typical electron temperature and density in the central cell and D-module are 30 eV and 2×10^{18} m^{-3}, and 1 ~ 30 eV and 0.01 ~ 1 $\times 10^{18}$ m^{-3}, respectively, before C-ECH injection.

The hydrogen plasma is produced and heated by ion cyclotron range of frequency wave from t = 51 to 440 ms, with additional hydrogen gas puffing for radiator gas in D-module from t = 50 to 450 ms at a pressure of 1200 mbar for the detached plasma experiment. C-ECH is injected at t = 300-310, and 320-330 ms in double pulse with a power of 130 kW. Figure 2 shows the time evolutions of diamagnetisms (red dotted line), line densities of the CC (CC-MIF, blue line) and EC-MIF (green line), indicating the double pulse C-ECH injection periods (yellow hatch). It is clearly confirmed that the electron line densities increased and diamagnetism slightly decreased with double pulse C-ECH injection. The electron densities and temperatures with and without C-ECH are approximately 6 eV and 2.3 × 10^{17} m^{-3}, and 3 eV and 1.2 × 10^{17} m^{-3}, respectively, in D-module (Fig. 3). The quick increase of ion flux with C-ECH injection was also observed (Fig. 4), which is comparable to the behavior of electron density. The plasma was in the detached condition before C-ECH injection. With C-ECH, the increase in electron density and temperature showed that the plasma transitioned to the attached condition. The transition time of detached to attached condition was approximately 1 ms which was calculated by a rise time of EC-MIF and it was considered suddenly increase of Hα intensity in HSCAM images (Fig. 5). The fall time of 1 ms in EC-MIF after cut of C-ECH shows the change from the attached state to the detached state. These changes were also observed in the second C-ECH pulse. The increase in ion flux and electron density with C-ECH injection indicates that the higher temperature electron flux increased plasma ionization, leading to a total increase in ion flux in the D-module. The intermittent higher electron density and temperature condition of the core plasma affects the D-module detached plasma condition, transitioning it to an attached plasma state during the C-ECH injection periods.

We revealed that the double pulse of higher temperature and density particle fluxes into the detached simulation plasma in D-module leads to higher ion flux. This double pulse higher electron temperature injection transitions the plasma from a detached to an attached condition twice. In the next step, we plan to use four-wavelength simultaneous measurements on HSCAM to investigate the overall hydrogen atomic and molecular processes in D-module. Additionally, we intend to conduct detailed emission spectroscopy of atoms and molecules along the magnetic field lines.

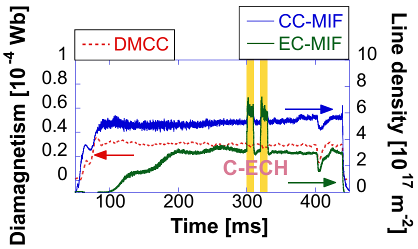

FIG. 2. Time evolutions of diamagnetisms (red dotted line), line densities in CC (blue line) and EC (green line) with C-ECH injection.

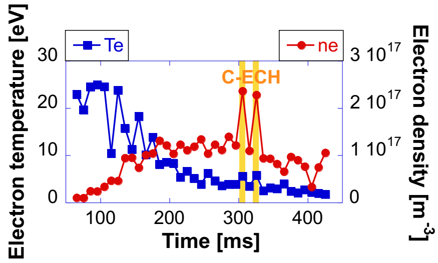

FIG. 3. Time evolutions of electron temperature (blue line) and electron density (red line) at ESP#3.

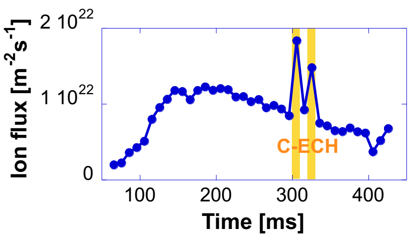

FIG. 4. Time evolution of ion flux at ESP #3.

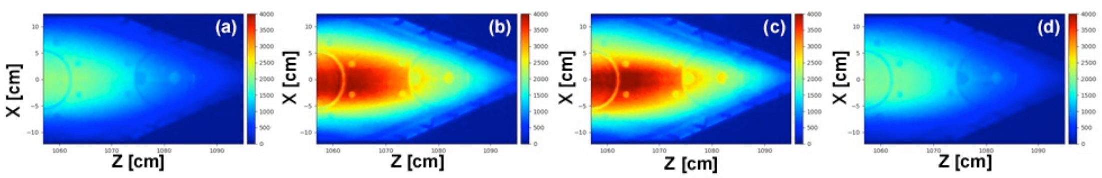

FIG. 5. Ha images at t = 300.4 ms (a), 301.2 ms (b), 310.0 ms (c), and 310.8 ms measured by HSCAM.

[1] M. Yoshikawa, et al., JINST, **18** (2023) C10006-1-7.
[2] M. Yoshikawa, et al., AIP advances, **14** (2024) 125324.